Potential use of APSIS-InSAR measures of the range of vertical surface motion to improve hazard assessment of peat landslides

Md. Tariqul Islam[1], Andrew V. Bradley[1], Andrew Sowter[2], Roxane Andersen[3], Chris Marshall[3], Mike Long[4], Mary C. Bourke[5], John Connolly[5], David J. Large[6]

[1] Department of Chemical and Environmental Engineering, Nottingham Geospatial Institute, University of Nottingham, UK
[2] Terra Motion Limited, Ingenuity Centre, Innovation Park, Jubilee Campus, University of Nottingham, UK
[3] Environmental Research Institute, University of the Highlands and Islands, Thurso, Scotland, UK
[4] School of Civil Engineering, University College Dublin, Ireland
[5] Department of Geography, Trinity College Dublin, Ireland
[6] Department of Chemical and Environmental Engineering, Faculty of Engineering, University of Nottingham, UK

SUMMARY

Peat landslides represent a notable natural hazard that is difficult to assess across complex blanket bog terrain. To aid the assessment of peat landslide susceptibility, we propose a new metric, the range of vertical surface motion (RVSM), quantified from time series data of surface motion measured using interferometric synthetic aperture radar (InSAR). Our expectation is that areas that are more susceptible to landslide will display a high RVSM that is indicative of high amplitude swelling and shrinking of the peat in response to changes in the volume of water stored in the peat over time. To test our hypothesis we examined the spatial distribution of high RVSM values that preceded three peat landslides in Ireland in 2020 and over a large area of blanket bog. We observed that high RVSM was closely associated with the known failures and with inferred points of initial failure, and that the areas of high RVSM were detectable up to two years in advance of failure. In the blanket bog landscape, high RVSM was associated with areas where landscape hydrology would favour thick peat and subsequent potential instability. We conclude that RVSM mapping has potential for refining national-scale assessments of peat landslide susceptibility.

KEY WORDS: bog breathing, Ireland, Meenbog, Mount Eagle, remote sensing, RVSM, Shass Mountain

INTRODUCTION

Peat landslides (slides, flows and bog bursts) are a significant natural hazard (Long & Jennings 2006, Dykes & Warburton 2008, Dykes & Jennings 2011, Long *et al.* 2011). In the United Kingdom (UK) and Ireland, this hazard is found particularly, although not exclusively, in areas of blanket peat where steeper slopes, complex topography and generally higher rates of landscape erosion are more likely to lead to peat instability (Warburton *et al.* 2003). Losses arising from peat landslides can be considerable and include both direct losses (e.g., carbon, biodiversity, water quality, infrastructure and farmland) and indirect losses (e.g., the trust of landowners and communities). With areas of blanket peatland being targeted for wind farm development (Lindsay & Bragg 2005, Scottish Government 2017), considerable government investment planned for extensive peatland restoration, and the increasing potential for peatland carbon trading, blanket bogs are at the forefront of policies to mitigate climate change in the UK and Ireland. It is therefore increasingly important that we understand this hazard and seek to avoid potential losses arising from peat landslides (Warburton *et al.* 2003, Lindsay & Bragg 2005, Long & Jennings 2006, Dykes & Warburton 2008, Dykes & Jennings 2011, Long *et al.* 2011, Scottish Government 2017).

Peat landslides can take many forms (Dykes & Warburton 2007a, 2008) but the underlying causes of increasing load, reduction in effective stress or removal of resisting forces are generally understood and common to all types of slope failure (Dykes & Kirk 2006). In the context of peat, hydrology is particularly important, as peat landslides are often associated with sudden changes in water input caused by intense rainfall (Warburton *et al.* 2004, Dykes & Warburton 2007a, 2007b). The response to such events is in turn determined by the internal structure of the peat and, in particular, the capacity for deep infiltration along macropores and peat pipes (Warburton *et al.* 2004) and tensional fissures (Bourke & Thorp 2005). Given that high magnitude rainfall events are already more likely due to global climate change and are predicted to increase further

by 2100 (Thompson *et al.* 2017, Davies *et al.* 2021), it is possible that peat landslides will become more frequent.

Several methods have been applied to landslide susceptibility assessment in a variety of locations on a range of substrates with success. The approach generally uses data-driven methods which explore the spatial relationships between existing landslides and a set of predisposing factors (e.g., van den Eeckhaut *et al*. 2012). Three dominant approaches are applied singly or in combination: statistical (e.g., Akgun *et al*. 2008, Devkota *et al*. 2013), numerical (e.g., Regmi *et al*. 2010, Pradhan 2011) and heuristic (e.g., Van Westen *et al*. 2003, Ruff & Czurda 2008). These methods have been tested predominantly on low-organic soils and rock, and determining landslide susceptibility and hazard in peatlands requires further work (Dykes & Kirk 2001, Warburton *et al.* 2004, Long & Jennings 2006). By way of example, a major peat landslide at Shass Mountain in 2020 (Figure 1, Table 1) occurred in an area of blanket bog that was classified on landslide hazard maps as having a moderately low to low susceptibility to failure (Geological Survey Ireland 2020). Reasons for difficulty in the prediction of this slide include a lack of information on local variations in the thickness (mass) of peat that are virtually impossible to detect without direct probing or ground penetrating radar assessment; poorly characterised geotechnical properties; and the unknown and complex internal and subsurface hydrology of the peat, which is also hard (if not impossible) to infer from surface features alone (Warburton *et al.* 2004, Dykes & Kirk 2006, Dykes & Warburton 2007b, Warburton 2020).

A possible improvement in our capacity to identify areas at greater risk of peat landslide comes from satellite remote sensing of surface motion. Remote sensing systems that focus on long-term monitoring of surface deformation may provide early warning of catastrophic slope failure. Synthetic aperture radar (SAR) and multi-temporal interferometry have specific advantages over optical wavelengths in locations, such as northwest Europe, that are subject to extended periods of cloud cover. In addition, they have large data swaths (at the regional scale), high spatial and temporal resolution (from days to weeks) and, importantly, a high precision of surface displacement measurements (mm–cm).

Surface motion of peat, sometimes referred to as 'bog breathing', is a natural response to changes in water storage (Howie & Hebda 2018). Changes in water storage are also responsible for changes in mass and effective stress (Price 2003), which are potential precursors to peat landslide. Areas that display large variations in water storage are likely to experience large variations in stress (Waddington *et al.* 2010) that may, in time, lead to failure of the peat structure via a variety of mechanisms such as liquefaction, basal sliding, shearing or fissuring. They are also likely to be areas where water naturally accumulates or discharges within the landscape and, hence, areas where peat started to accumulate earlier and is therefore thicker (Winter 2000, 2001; Winter & LaBaugh 2003) and potentially closer to its limit of mechanical stability (Large *et al.* 2021) within the blanket bog. The processes leading to failure should occur under natural conditions as a consequence of repeated and irreversible deformation of the peat structure and may be exacerbated as a consequence of the development or modification of the peatland.

Detailed time series of peatland surface heights, at high spatial (20 m) and temporal (up to 6 days) resolution, can be quantified with the Advanced Pixel System using the Intermittent SBAS (APSIS) interferometric SAR (InSAR) technique. Formerly known as the Intermittent Small Baseline Subset - ISBAS (Sowter *et al.* 2013), this method uses radar images from the Sentinel-1 satellites of Copernicus, the European Union's Earth Observation programme (https://www.copernicus.eu/en). Of particular note, the APSIS-InSAR technique closely monitors the coherence between many pairs of images and, through a detailed analysis, is able to provide near-continuous surface coverage even over densely forested areas (Sowter *et al.* 2013, Gee *et al.* 2017, Novellino *et al.* 2017). The APSIS-InSAR time series contains signals that display a clear response to changes in the quantity of water stored within the peat (Alshammari *et al.* 2020). Using these signals, we should be able to identify areas that display unusually large vertical ranges of surface motion in response to changes in water storage.

We hypothesise that peatlands which display a large range of vertical surface motion will have an increased likelihood of peat landslide. To test this hypothesis, we derived a new measure from the APSIS InSAR time series, namely the range of vertical surface motion (RVSM) measured in mm. The objectives of this study are: (1) to determine whether high RVSM is spatially contiguous (i.e., not random noise) and if it preceded three peat landslides that occurred in blanket bog in Ireland during 2020 (Figure 1, Table 1); (2) to understand the spatial correlation between high RVSM values and position within the blanket bog landscape; and (3) to compare our results with the current landslide hazard risk assessment and the locations of historical peat landslides in this area (Geological Survey Ireland 2021).

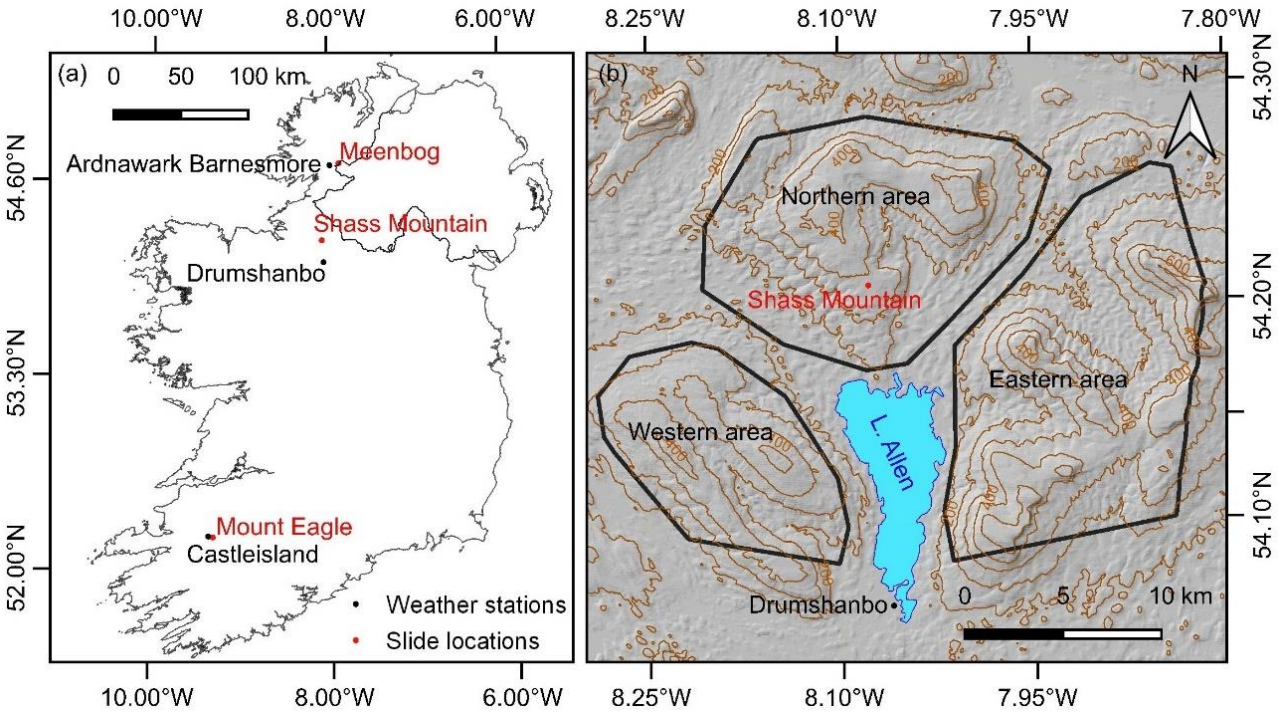

Figure 1. Maps of Ireland showing (a) the locations of the three peat failures analysed (red dots) and their closest weather stations (black dots), and (b) the investigation sites on upland areas with blanket bog around Lough Allen that were selected to demonstrate the mapping of peat slide risks. Contour interval 100 m.

Table 1. General characteristics and information relevant to the three peat slides analysed. Altitude and slope are derived from 30 m resolution SRTM data (Farr *et al.* 2007). Landslide susceptibility is taken from Geological Survey Ireland (2021).

Slide	Mount Eagle	Shass Mountain	Meenbog
Slide date	15 Nov 2020	28 Jun 2020	13 Nov 2020
Slide area	~ 6 ha	~7 ha	~3 ha
Centre point	52° 13' 34.96" N -9° 18' 18.65" E	54° 12' 26.45" N -8° 04' 40.48" E	54° 43' 8.97" N -7° 52' 24.01" E
Motion analysis	06 Dec 2018 – 13 Nov 2020	07 Jun 2019 – 25 Jun 2020	07 Dec 2018 – 08 Nov 2020
Peatland type	Blanket bog	Blanket bog	Blanket bog
Vegetation, human disturbance	Forestry plantation	Open peatland with forestry; dense drainage network at top of catchment.	Open peatland and felled forestry plantation; wind farm access road crosses slide.
Altitude	335–432 m a.s.l.	262–286 m a.s.l.	247–265 m a.s.l.
Slope	Gentle to steep 8.5° (mean), ~2–15° (range)	Gentle to moderate 2.7° (mean), ~1–7° (range)	Very gentle to gentle 2.5° (mean), ~1–4° (range)
Aspect	SE to NW	NE to SW	SW to NE
Landslide susceptibility	High and moderately high	Low and moderately low	Low and moderately low
Nearest weather station	Castleisland 52° 13' 58.8" N -9° 21' 21.6" E	Drumshanbo 54° 03' 39.6" N -8° 03' 39.6" E	Ardnawark Barnesmore 54° 42' 25.2" N -7° 58' 40.8" E

METHODS

For this study we determined the RVSM for an area of 1 km^2 surrounding each of three peat landslides in blanket bog that occurred in Ireland during 2020 (Figure 1a). These are, from south to north, Mount Eagle in County Kerry, Shass Mountain in County Leitrim (Connolly *et al.* 2021) and Meenbog in County Donegal. Site details, characteristics and topography are summarised in Table 1. To understand the general association between high RVSM, topography and areas known to be susceptible to peat landslides, the RVSM was also determined for three areas of upland blanket bog around Lough Allen (Figure 1b). The latter three areas were chosen because they were typical examples of upland blanket bog for the region, contained a large number of historical peat failures and, from a processing point of view, the data were easily generated from a single satellite radar scene around the Shass Mountain study location. We termed them the Eastern (~187.8 km^2, altitude 60–640 m a.s.l.), Northern (~161.3 km^2, altitude 50–440 m a.s.l., which includes the Shass Mountain landslide) and Western (~92.7 km^2, altitude 70–440 m a.s.l.) areas. In all areas, the RVSM was determined at a pixel resolution of 20 m.

In addition, data for historical peat landslides and the current landslide hazard classification were obtained for all the study areas from Geological Survey Ireland (2021). Daily precipitation data (Met Éireann 2021) were obtained from the nearest weather stations to the three peat landslide areas: CastleIsland for the Mount Eagle site; Drumshanbo for the Shass Mountain site; and Ardnawark-Barnesmore for the Meenbog site (Table 1).

Surface motion time series

To derive the surface motion, we used satellite data from Sentinel-1A and -1B SAR satellites archived on the European Space Agency Copernicus Open Access Hub (https://scihub.copernicus.eu; Table 2). Differential InSAR (DInSAR) - the process of detecting phase changes in the radar Line-Of-Sight (LOS) associated with surface displacement between satellite overpasses on different dates - was applied using these data with the APSIS technique (Sowter *et al.* 2013). The APSIS technique contains an adapted version of the established SBAS DInSAR time series algorithm (Berardino *et al.* 2002) to improve the density and spatial distribution of survey points to return measurements in vegetated areas (Bateson *et al.* 2015, Cigna & Sowter 2017). Other DInSAR processing algorithms habitually struggle due to

Table 2. Details of the Sentinel-1 radar images and APSIS-InSAR processing parameters.

Study sites	Mount Eagle	Shass Mountain and Northern, Eastern and Western areas	Meenbog
Orbit	ascending path 74 descending path 23	ascending path 74 descending path 23	ascending path 74 descending path 23
Time series (6-day interval)	06 Dec 2018 – 13 Nov 2020	07 Jun 2019 – 25 Jun 2020	07 Dec 2018 – 08 Nov 2020
Temporal gaps	Complete	Complete	24 May 2019, 02 Nov 2020
Stable reference point	Castleisland 52° 13' 48" N -9° 21' 36" E	Drumkeeran 54° 10' 07" N -8° 08' 32" E	Ballybofey 54° 48' 00" N -7° 46' 12" E
Maximum perpendicular baseline (m)	150	100	150
Temporal separation (days)	183	365	183
Total interferograms	ascending 2990 descending 3002	ascending 1631 descending 1660	ascending 2870 descending 2983
Coherence threshold	0.45	0.45	0.45
Point threshold	ascending 1350 descending 1650	ascending 760 descending 875	ascending 855 descending 972

incoherence outside urban areas (Gong *et al.* 2016, Osmanoğlu *et al.* 2016). The APSIS algorithm was implemented using Terra Motion Limited's in-house Punnet software, which covers all aspects of processing from the co-registration of SLC (Single Look Complex) data to the generation of time series (Sowter *et al.* 2016). For each site, the horizontal baselines, temporal separation, coherence and point thresholds and the location of the stable reference point were set for the APSIS processing (Table 2). Phase unwrapping was implemented using an in-house implementation of the SNAPHU algorithm (Chen & Zebker 2001). Using APSIS, the time series of LOS motion (m) was calculated and georeferenced at approximately 20 m resolution. Two APSIS LOS surveys were applied to each site: one from an ascending orbit and one from a descending orbit. As SAR is an oblique sensor, and with a range of incidence angles of 29–45 degrees for the Sentinel-1 geometry, this allows us to resolve the vertical component of the motion more perfectly through an opposite-side stereo analysis. Unfortunately, a stereo analysis from two positions in orbit is only able to resolve a single E–W lateral component of motion. So, despite lateral movement being a potentially important indicator of landslides, only the consistently measured vertical component was used in this study. Layover and shadow masks were calculated through image simulation and applied to the resulting products to remove any anomalous areas within each survey (Schreier 1993).

The three study sites and regional upland data were selected from these data as smaller sub-scenes. Any temporal data gaps were filled using linear interpolation across the gap (Table 2). No time series were calculated for pixels for which coherence could not be resolved, and these were not filled.

To determine the benefits of enhanced processing, the RVSM in the time series was measured on two forms of the time series. The first form was simple processing of the time series using means deduction to rescale each time series around zero. This is referred to as the standard APSIS data analysis. The second form - a more complex processing of the time series - was performed using Multichannel Singular Spectrum Analysis (MSSA) via the SSA-MTM toolkit (Ghil *et al.* 2002, SPECTRA 2021), which was used to remove longer term (climate, subsidence) and seasonal (evapotranspiration) trends. This was applied because long-term trends, particularly long-term subsidence, could generate a high RVSM without the peat being responsive to the shorter-term weather patterns that appear to be more closely associated with peat landslides. For the MSSA analysis, covariance was calculated after channel reduction with Principal Component Analysis (PCA). Using a window of three months to capture precipitation events, rather than longer-term annual cycles related to annual trends in evapotranspiration (Bradley *et al.* 2022), we calculated the first ten PCA channels and 20 Empirical Orthogonal Functions (EOFs) to identify long term oscillations in the time series. We found that most of the variance was in EOF 1, and that this related to long-term trends in the time series. This was removed and the time series reconstructed using the remaining EOFs 2–20. This reconstructed time series retained peaks and troughs on a timeframe of 18–90 days which enabled us to consider the response to variations in precipitation on a similar timeframe.

Analysis of time series

There were approximately 2500 motion time series within the 1-km^2 area around each peat slide (Figure 2). For each site, the RVSM was measured as the difference between maximum and minimum values in the time series during a defined period preceding the landslide event. In order to determine appropriate timeframes for these measures, the RVSM was measured at 1–6, 1–12 and 13–24 months prior to the Meenbog and Mount Eagle landslides. For Shass Mountain and the blanket bogs around Lough Allen, 13–24 months' data were not available due to resource limitations. For the three areas of blanket bog surrounding Lough Allen the RVSM was determined for the 1–12 month period prior to the Shass Mountain landslide. For classification purposes, we defined high RVSM values as exceeding the 80th percentile and classified the following percentile ranges: > 95 % (very high), 90–95 % (high), 85–90 % (moderate), 80–85 % (low) and < 80 % (negligible) (Figures 3, 4). This percentile range was chosen based on a preliminary analysis of the percentile range that delineated a discrete high RVSM area within the Shass Mountain landslide. To improve visualisation, the classified RVSM maps of County Leitrim area were filtered by passing a 3X3 majority filter over them using ESRI ArcGIS.

To illustrate the differences and variability in time series characteristics and evaluate the response to precipitation, surface motion time series for a high RVSM area within each landslide area and a low RVSM area from adjacent blanket bog that did not experience failure were selected (points F and P, respectively, in Figure 2). Standard deviations for each of the time series were obtained by averaging the time series for pixels within a 3 × 3 pixel window surrounding and including the central pixel (Figure 5). Linear regression of precipitation versus mean surface motion was undertaken on normalised

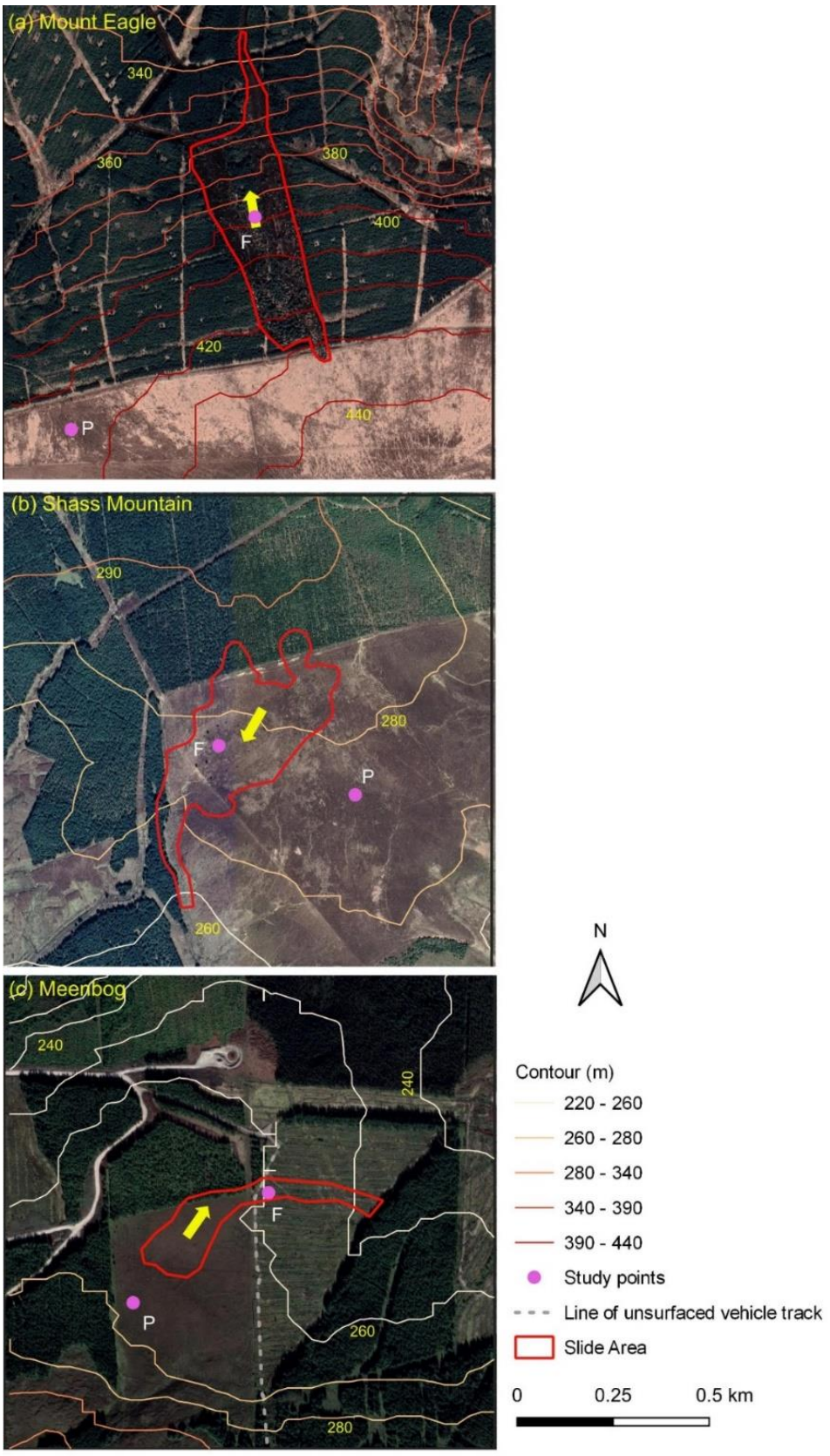

Figure 2. Google Earth aerial images (pre-failure) of the Mount Eagle, Shass Mountain (RPS 2020; see also Figures 9 and 10) and Meenbog study sites with superposed contours (10 m interval). Dark green areas are forestry plantations and light brown areas are mostly blanket bog. For each site, the red polygon outlines the area of peat failure and the yellow arrow indicates the direction of sliding. Also shown are the locations of the selected RVSM examples of peatland outside the failure area (P) and within the failure area (F).

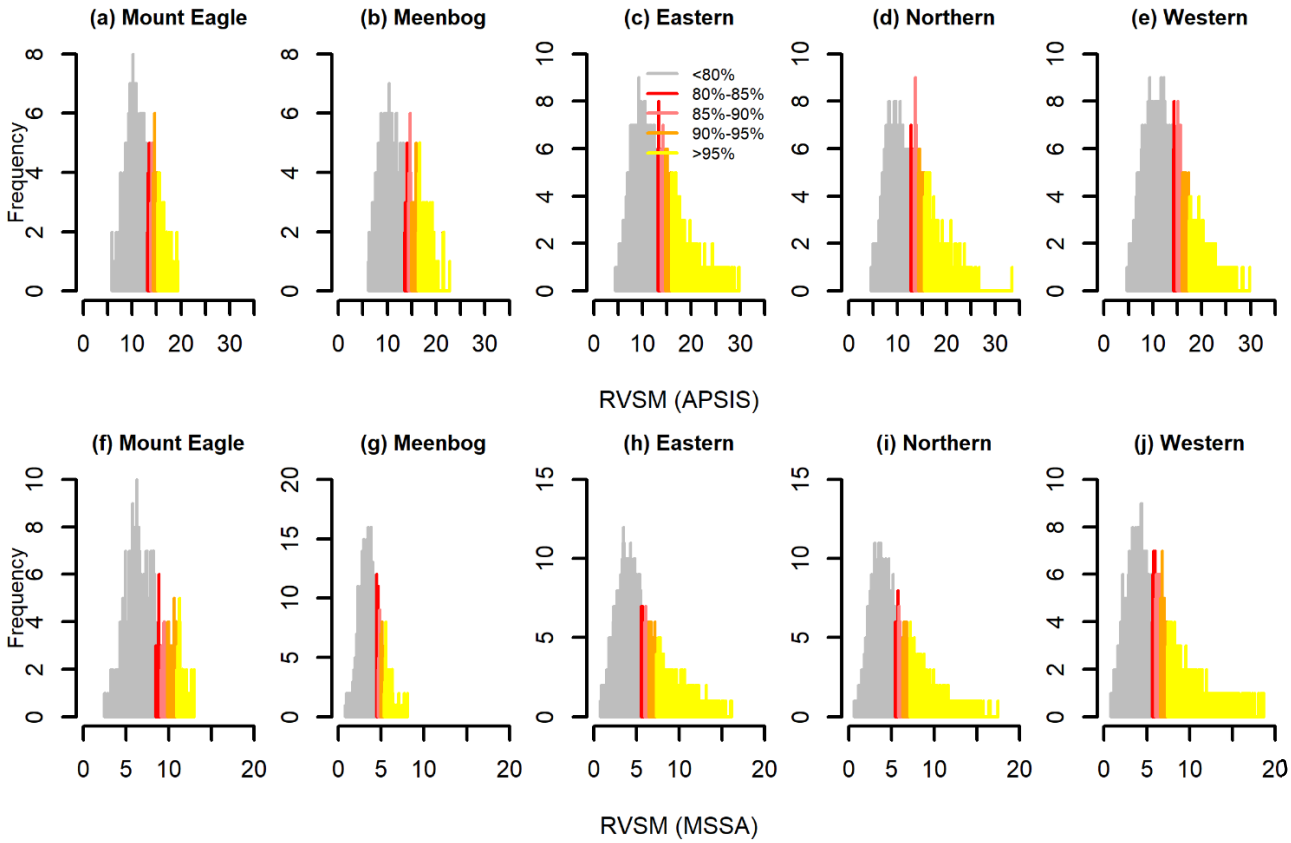

Figure 3. Frequency distributions of RVSM (mm) for 1–12 months for the Mount Eagle and Meenbog study sites and the regional upland areas, showing the percentile dynamic ranges selected to discriminate extreme values in Figure 4. The Shass Mountain study site is included in the Northern upland area. Note that the classification for Shass Mountain was based on the distribution for the whole of the Northern area.

data (mean subtraction and then divided by standard deviation) for the two locations (F and P points; Figure 6).

RESULTS AND INTERPRETATION

The spatial variation of RVSM is described and interpreted separately for each study site below.

Mount Eagle

An area of high RVSM occurs in the middle of the peat landslide area where a convex slope changes from low gradient (upslope) to a steeper gradient (downslope) within a forest plantation. This area also corresponds closely to a narrow gap in the forestry, presumably positioned to allow access (Figure 4a-d-g-j-m-p). An area of high RVSM also occurs on low angle slopes above the landslide. The area of high RVSM is clearly resolved in MSSA data and poorly resolved in the Standard APSIS data for all periods of measurement. The area of high RVSM within the landslide is clearly resolved 24–13 months prior to the landslide. Average time series from high RVSM areas within the area of peat landslide clearly display higher amplitude oscillations than low RVSM areas with apparently similar topographic setting outside the landslide area (Figure 2a, 5a-b). Comparison with precipitation data (Figure 5a-b, Figure 6a-b) indicates a significant correlation between precipitation and surface motion for the high RVSM area within the landslide area and a significant negative correlation for the chosen area of low RVSM outside the landslide area.

Within the landslide area upslope of the area of high RVSM the predominant landslide pattern, seen by detailed examination of available optical images, appears to have been retrogressive translational failure extending uphill beyond the limit of the forestry plantation (Figure 2a). We therefore speculate that the high amplitude area is close to the point where the landslide initiated, an interpretation that is consistent with that of Dykes (2022). The positive correlation between the precipitation record and surface motion within the area of landslide indicates that precipitation has influenced the high amplitude response and is therefore likely to have

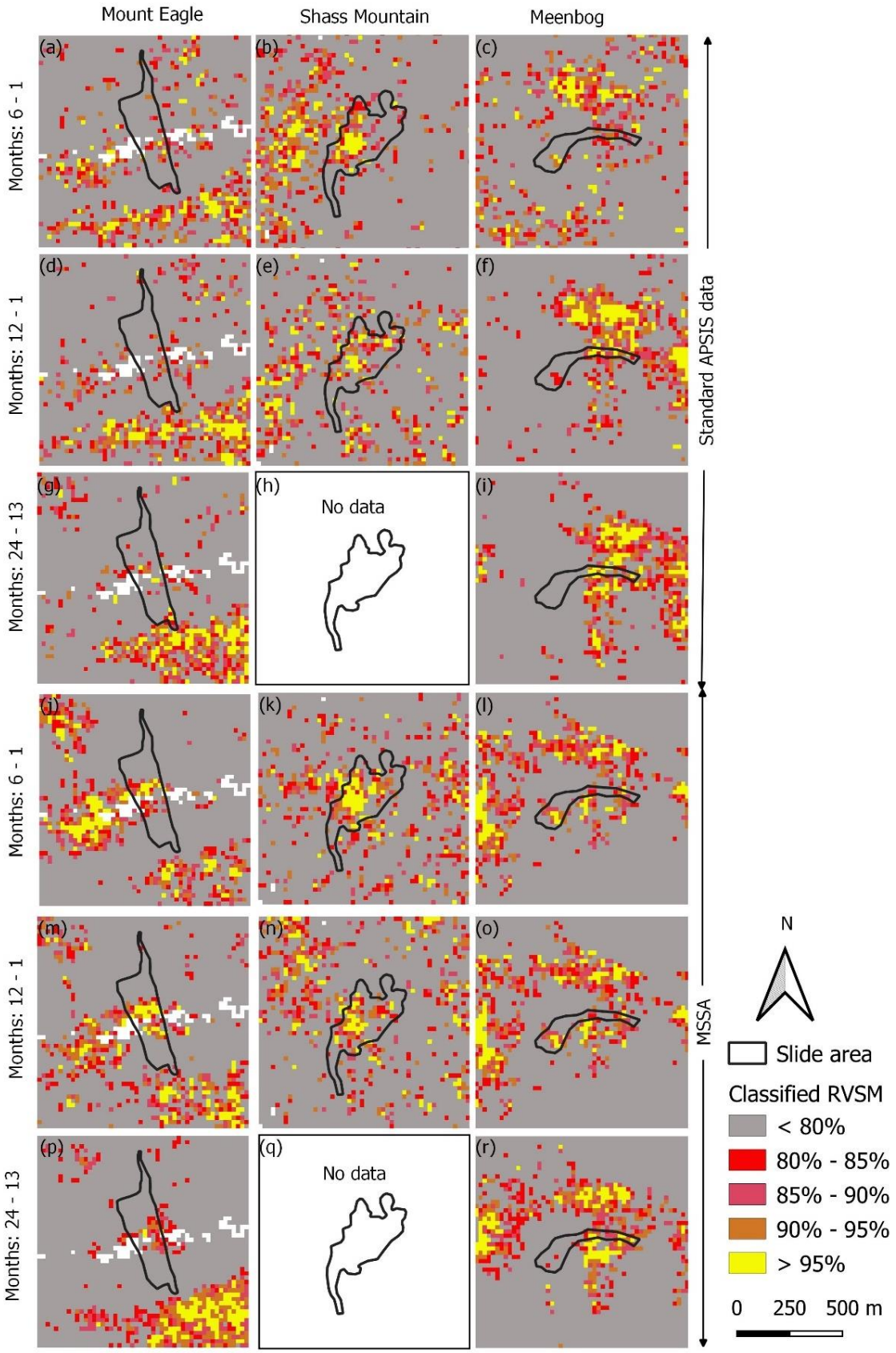

Figure 4. RVSM for the three slide sites shown as percentiles, for standard APSIS (a–i) and MSSA (j–r) data, for the six (a–c, j–l) and twelve (d–f, m–o) month periods immediately preceding the slide, and for the twelve month period (g–i, p–r) ending one year ahead of the slide. White areas indicate no data.

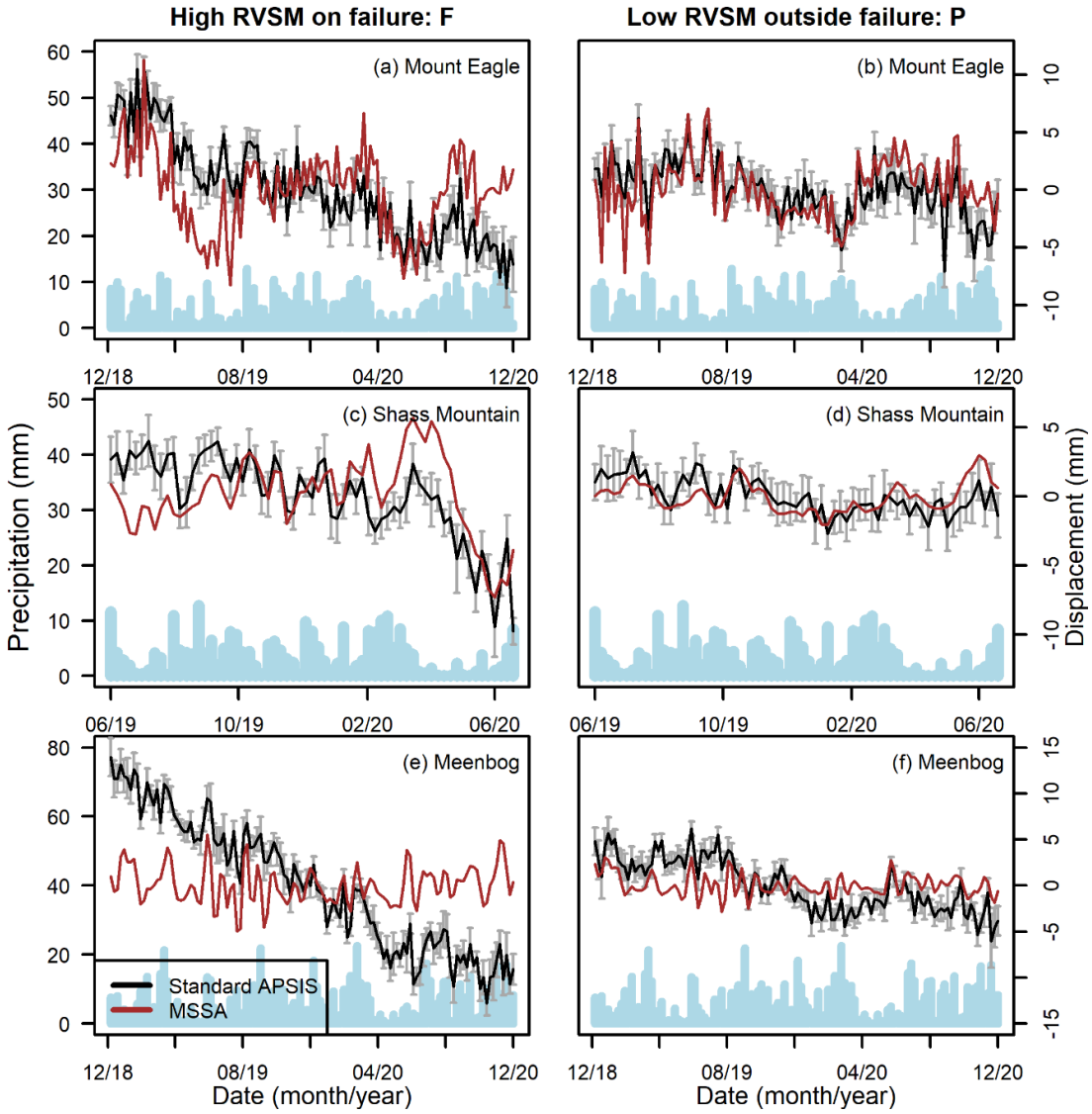

Figure 5. Time series of daily precipitation (light blue histogram), the average surface motion for an area of high RVSM (F) within the area of the peat slide, and for an area of low RVSM (P) in neighbouring blanket bog outside the area of the peat slide (Figure 2), for the Mount Eagle (a–b), Shass Mountain (c–d) and Meenbog slides (e–f). Surface motion from both the standard APSIS and the MSSA (upscaled ×2 for visualisation) results is shown.

directly influenced the landslide at this point. It is notable that, on such steep slopes, sub-peat soils and hydrology have been noted as playing a significant part in the failure mechanism (Dykes & Warburton 2007b, 2008). However, in the absence of detailed field evidence, this is speculative.

Shass Mountain

At Shass Mountain (Figure 4b-e-k-n), the landslide has two branches extending upslope towards and into the adjacent forest plantation and a distinct area with high RVSM occurs within the western branch of the landslide (Figure 2b). Areas with high RVSM also occur outside of this area with the most notable instance in the forestry to the west of the landslide (Figure 2b). The areas of high RVSM are clearly delineated in both the 1–6 months and 1–12 months standard APSIS and MSSA data (Figure 4b-e-k-n). Average time series from high RVSM areas within the area of peat landslide clearly display higher amplitude oscillations than low RVSM areas outside the landslide area. Comparison with precipitation data (Figures 5c–d, 6c–d) indicates no correlation between precipitation and surface motion for the high RVSM area within the landslide area and a negative correlation for the chosen area of low RVSM outside the landslide area. However, inspection of the time series shows what may be a lagged response between

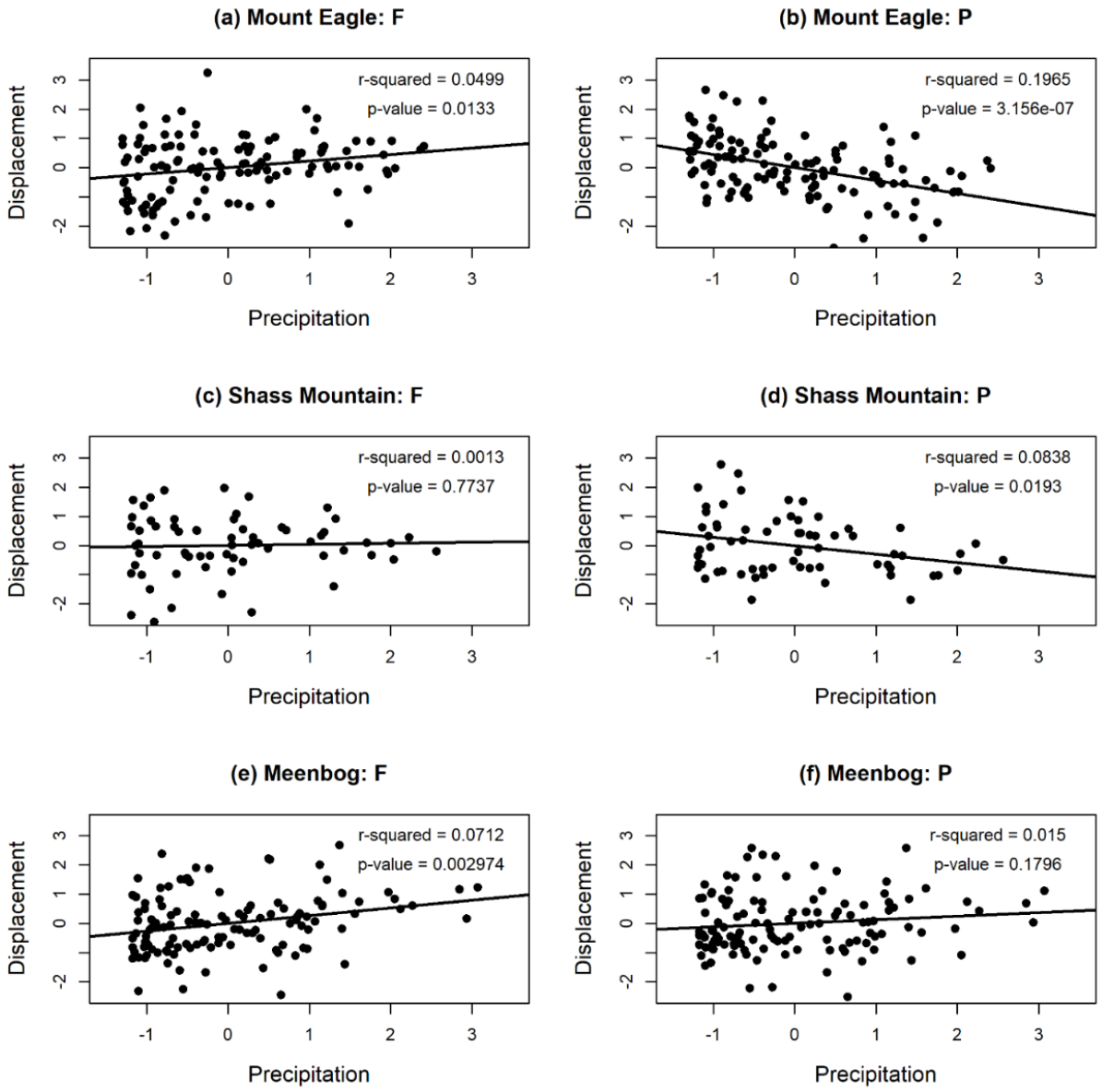

Figure 6. Scatter plots of normalised precipitation and vertical surface motion (MSSA data) time series within the peat slide (F) and on nearby blanket bog (P) (see Figure 2), for the Mount Eagle (a–b), Shass Mountain (c–d) and Meenbog slides (e–f). Linear-regression is shown with r-squared and p-value.

surface motion and rainfall within the landslide area (Figure 5c-d). The lagged response is most obvious between the intense period of precipitation in February to March 2020 and the subsequent surface motion (Figure 5c).

At Shass Mountain the position of the high RVSM area within the landslide is known from SAR imagery to correspond to the area where the peat landslide is hypothesised to have initiated before propagating retrogressively into the eastern arm of the landslide (Connolly *et al*. 2021, Dykes 2022). The lagged response of surface motion to precipitation events may indicate that water was accumulating within the high RVSM area. This would be consistent with this area being the upslope extension of a natural drainage line, possibly a zone of seepage prior to failure. Indeed, drainage analysis carried out in ArcGIS using the Flow Accumulation tool with a high-resolution DSM dataset from 2017 indicates a converging drainage pattern that suggests this. Post-landslide ground observations reported large rafts of peat super-elevated approximately 2 m above the pre-slide surface on the bank opposite this convergence (Figure 7a). This suggests a highly fluidised peat that failed in an abrupt manner. This mode of failure would be aided by heterogenous sub-surface water accumulation above the convergence point and may have been accentuated by the presence of peat

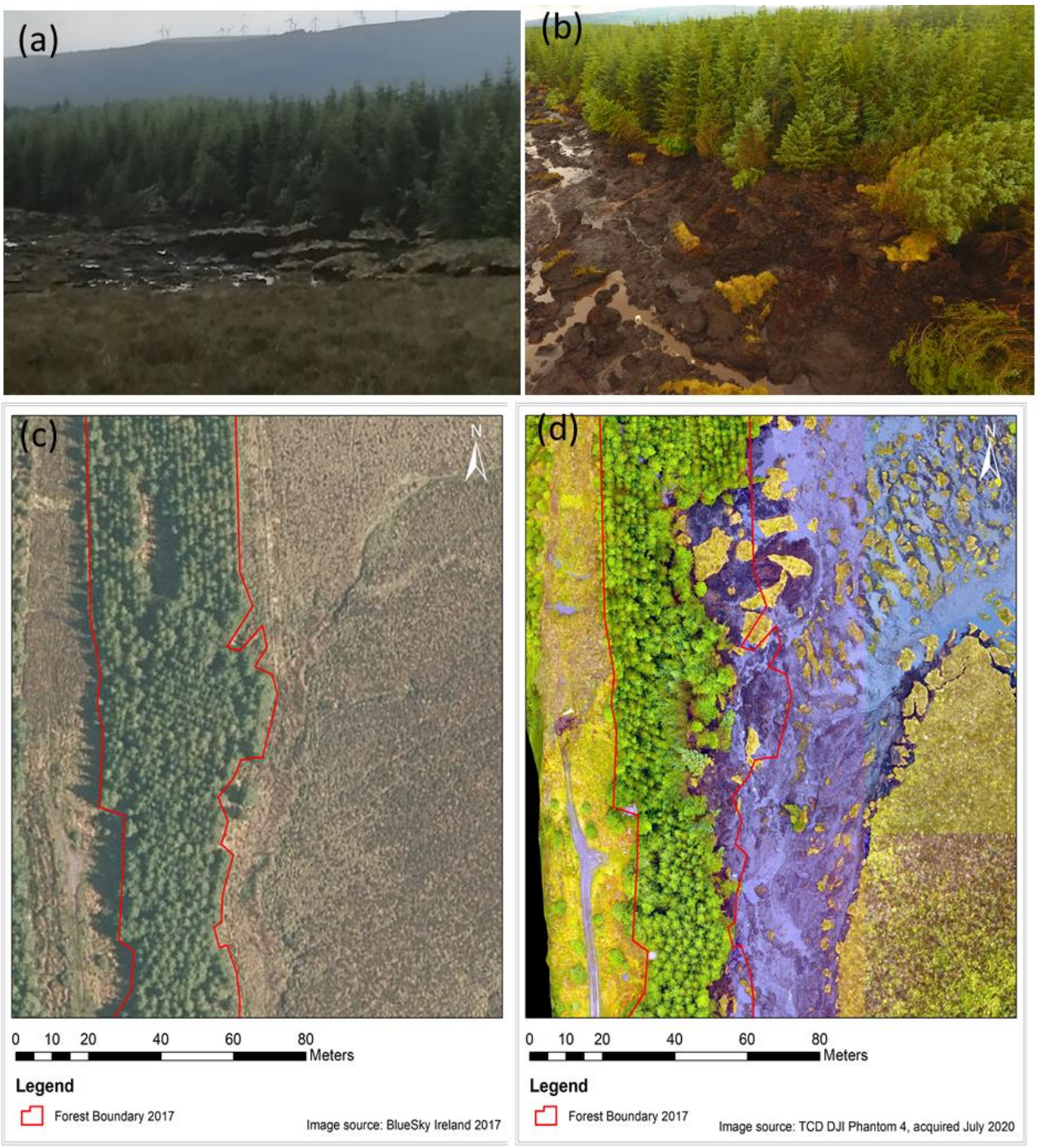

Figure 7. Images of the peat landslide area on Shass Mountain illustrating the impact of the landslide on the forest margin: (a) slabs of peat stack up against the forest edge; (b) trees along the forest edge felled by the force of the landslide; (c) outline of the forest edge before the landslide; (d) outline of the forest edge after the landslide illustrates the extent of the area in which trees were felled by the force of the landslide.

pipes and drainage from the nearby forest. The force of the moving peat was sufficient to knock down trees (Figure 7b). The progress of the slide at Shass Mountain is illustrated in Figure 8. The outline of the final slide area (generalised) from RPS (2020) was considered.

Meenbog

In the MSSA data and in some of the standard APSIS data an area of high RVSM is clearly defined in the lower part of the peat landslide area starting at the edge of the forestry plantation (Figure 2c, 4c-f-i-o-r). An area of high RVSM is also clearly defined in the

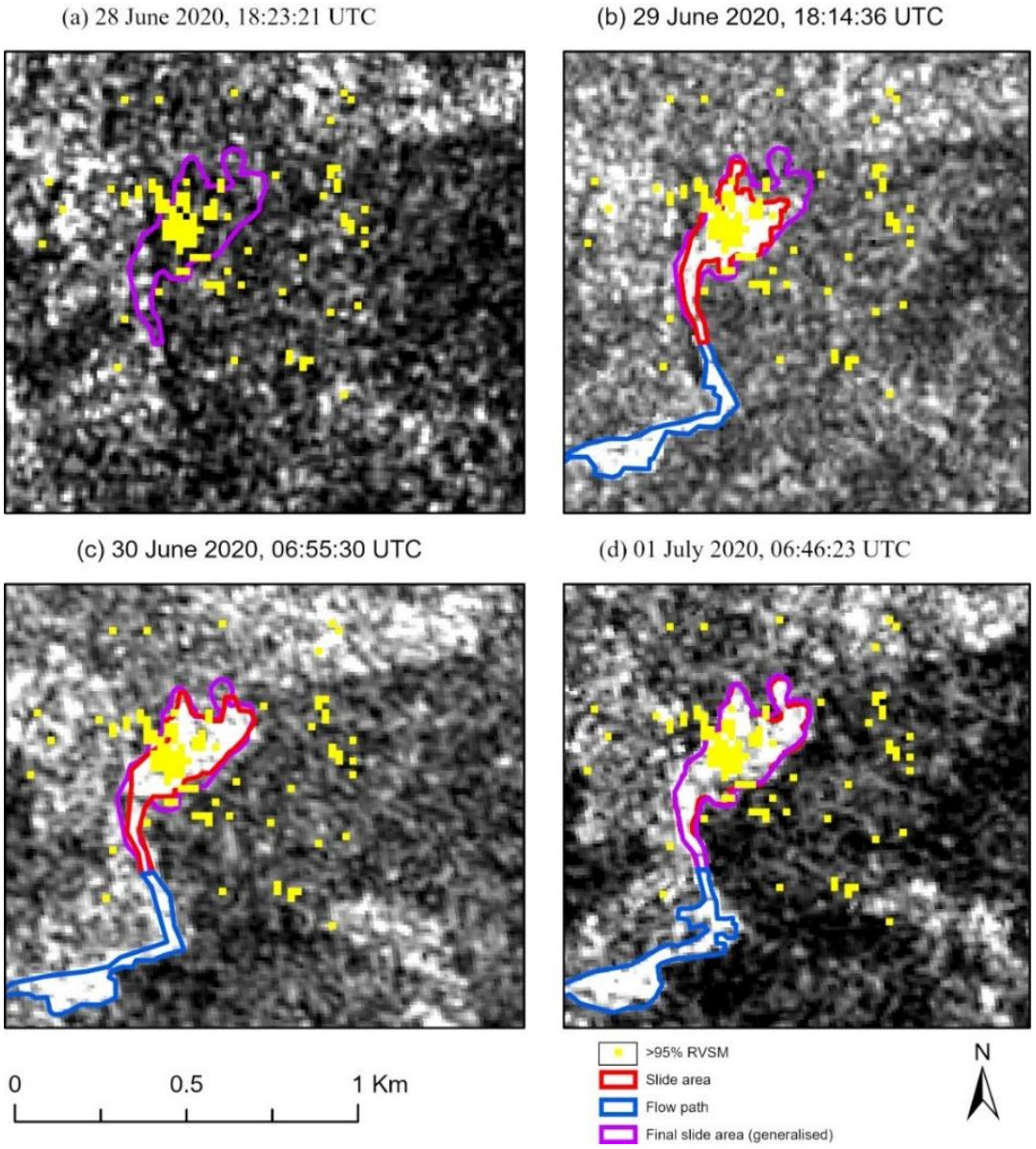

Figure 8. VV polarised ESA Sentinel 1 synthetic aperture radar amplitude illustrating the progression of the Shass Mountain landslide relative to areas of high RVSM: (a) pre landslide on 28 June; (b) 29 June; (c) 30 June; and (d) 01 July 2020. The area of high RVSM is the area exceeding the 95th percentile derived from MSSA data 1–6 months prior to the landslide.

upper part of the landslide in both the MSSA with standard APSIS data in the period 1–6 months prior to the failure (Figures 1, 4c). In the surrounding peatland distinct areas of high RVSM also occur at the head of a drainage line to the north of the landslide and over gently sloping ground to the west of the landslide. In the period 13–24 months pre-landslide an area of high RVSM is clearly defined in both the standard APSIS and MSSA data in the lower part of the landslide and there is some evidence of high RVSM in the upper part of the landslide in the MSSA data (Figure 4i-r). Average time series from high RVSM areas within the area of peat landslide clearly display higher amplitude oscillations than those from low RVSM areas outside the landslide area (Figure 5e-f). Comparison with precipitation data (Figure 5e-f, 6e-f) indicates no correlation between precipitation and surface motion within the high RVSM area within the landslide area and a negative correlation within the chosen area of low RVSM outside the landslide area (Figure 5f, 6f).

At Meenbog, the main area of high RVSM occurs in the lower part of the landslide area within an area of forestry and may be associated with the upslope extension of a natural drainage line. Above the area of high RVSM the predominant landslide mechanism

appears to have been translational failure, so we anticipate that the break point is very close to or below where the wind turbine access road (Figure 2c, 4c-f-i-l-o-r) that runs along the top of the high RVSM area, an interpretation that is consistent with that of Dykes (2022). The close correspondence between precipitation and the response of the surface motion time series indicates that rapid infiltration and concentration along flow pathways may have been a major cause of the surface motion. It has also been observed that access roads on peat can create barriers to flow that can accentuate movement both above and below the road (Marshall *et al.* 2021).

Regional blanket bog sites

RVSM data from the three large areas of blanket bog (Figures 9 and 10) in addition to the observations made in the vicinity of the known landslides reveals a number of distinct and repeated topographic associations. Areas of high RVSM are frequently associated with low gradients, areas of seepage including breaks in slope, saddles, and the apparent upslope continuation of drainage lines and slopes with a N or NE aspect (Figure 10). Comparison of the distribution of known peat landslides to areas with high RVSM shows a distinct correspondence (Figure 9) and in some areas high RVSM is closely associated with clusters of peat landslides (e.g., Figure 10r). Comparison of RVSM determined from the standard APSIS data to that determined from the MSSA data indicates that areas of high RVSM are generally more discrete and show more clearly defined topographic associations when the MSSA data is used. While we have sought to illustrate systematic associations between high RVSM and topography it is clearly not possible to account for every instance where a high RVSM is observed without detailed analysis of the field conditions, hydrology, geology, etc.

The association of high RVSM with low-angle slopes, breaks in slope, and upslope extensions of drainage lines is consistent with areas that will be naturally wetter on account of poor drainage, enhanced infiltration and seepage (Winter 2001). These are also the areas where peat accumulation should have been initiated earlier (Winter 2001) and locally thicker peat could be expected. The association between high RVSM and slopes with a N to NE aspect has been noted in blanket bog and associated steeper terrain in northern Scotland (Marshall *et al.* 2021), where it was thought that lower insolation on northward-facing slopes made them generally wetter.

The better definition achieved using the MSSA data is not surprising as the standard APSIS data will contain longer-term (multiannual) trends related to climate or peat subsidence, which can determine the measured range of motion. It may be that areas which are naturally more dynamic will tend to display greater long-term ranges of surface motion; however, this need not be the case. The reverse may also be true - that areas which should rationally be expected to have a high RVSM may not. Possible reasons for this may be the natural formation of drainage lines, e.g., peat pipes or sub-peat drainage, that limit the accumulation of water within the peat.

DISCUSSION

The key finding is that in all three study areas the initial area of failure appears to be clearly associated with areas displaying high RVSM, thereby confirming our hypothesis. It can therefore be inferred that for the two sites (Meenbog and Shass Mountain) that were given a moderately low to low landslide susceptibility classification, RVSM had the potential to enhance both susceptibility and hazard mapping. In addition to this, at the regional scale, high RVSM occurs in areas where water will logically accumulate and thick peat is likely to have formed. Intuitively for a given slope, these areas should present a greater potential hazard on account of greater mass and higher pore water pressures. Although, explaining all areas of higher RVSM is beyond the scope of this study, the association of high RVSM with areas of known landslide and the logical association with areas of potentially greater hazard within a landscape demonstrates that it has the potential to improve peat landslide susceptibility mapping. In particular, the data lend strength to the inferred location of failure initiation, enabling identification of high-risk locations and targeting of mitigation measures.

A positive correlation between surface motion and precipitation is obvious in areas of high RVSM at Mount Eagle and Meenbog and there is possibly a lagged correlation at Shass Mountain. This is not surprising as infiltration, lateral flow and storage within and below peatland is likely to be variable (Holden 2005). A rapid direct response to a period of intense precipitation indicates relatively rapid infiltration, possibly due to artificial drainage and/or lateral flow. A significant lag between precipitation and surface motion may indicate the accumulation of water from a greater area, possibly with longer flow paths or slower groundwater discharge into the peat and/or notable water storage within or under the peat body. An interesting observation that merits future investigation is the significant inverse correlation observed in areas of low RVSM at Mount Eagle and

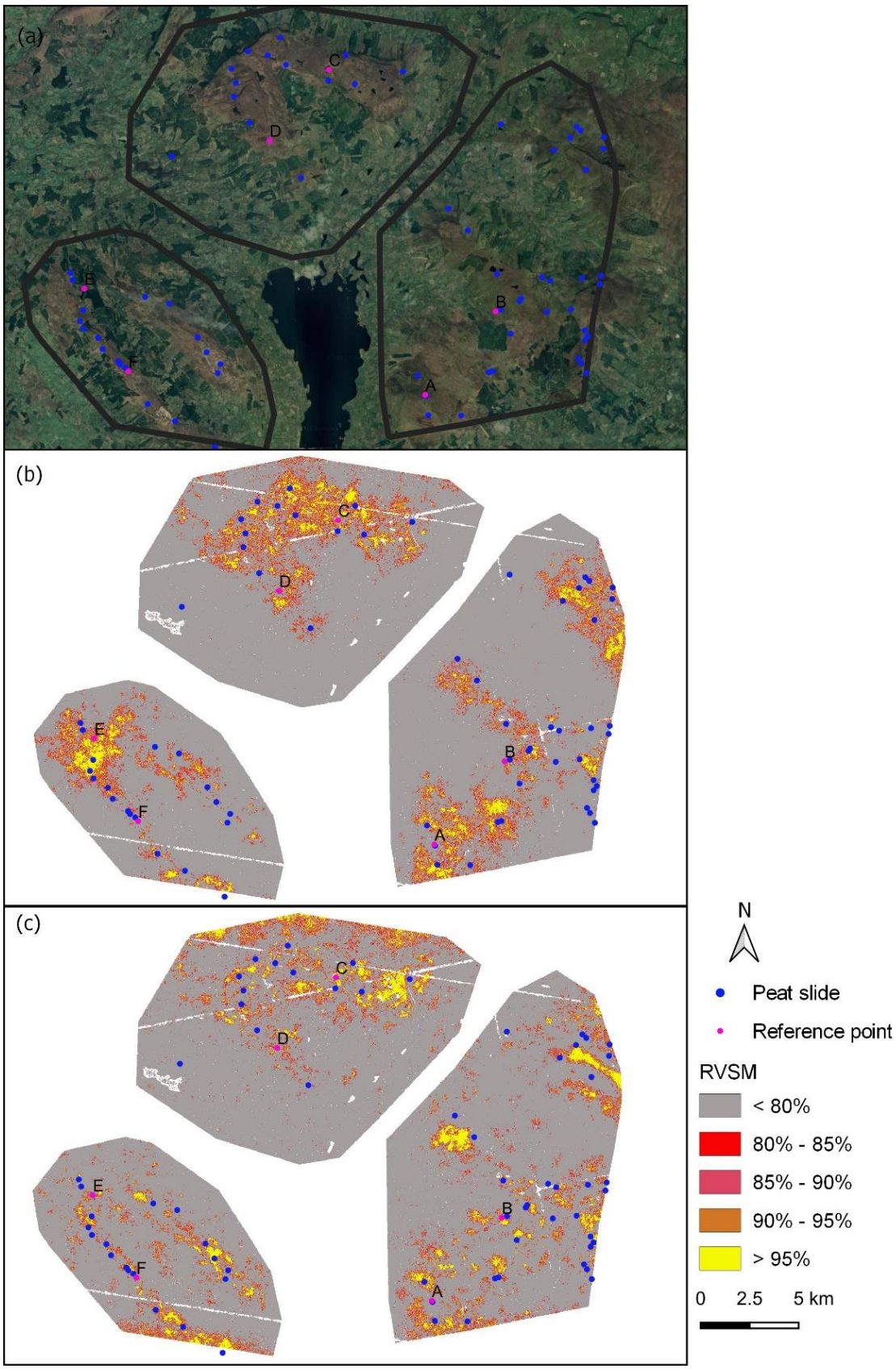

Figure 9. (a) Google Earth image showing the locations of historical peat slides (blue dots) in the upland study areas (Northern, Eastern and Western) around Lough Allen. The middle and lower panes show one-year RVSM of (b) standard APSIS data and (c) MSSA data, as percentiles. Areas around the reference points (A–F) are expanded for detailed comparison in Figure 10 (Geological Survey Ireland 2021).

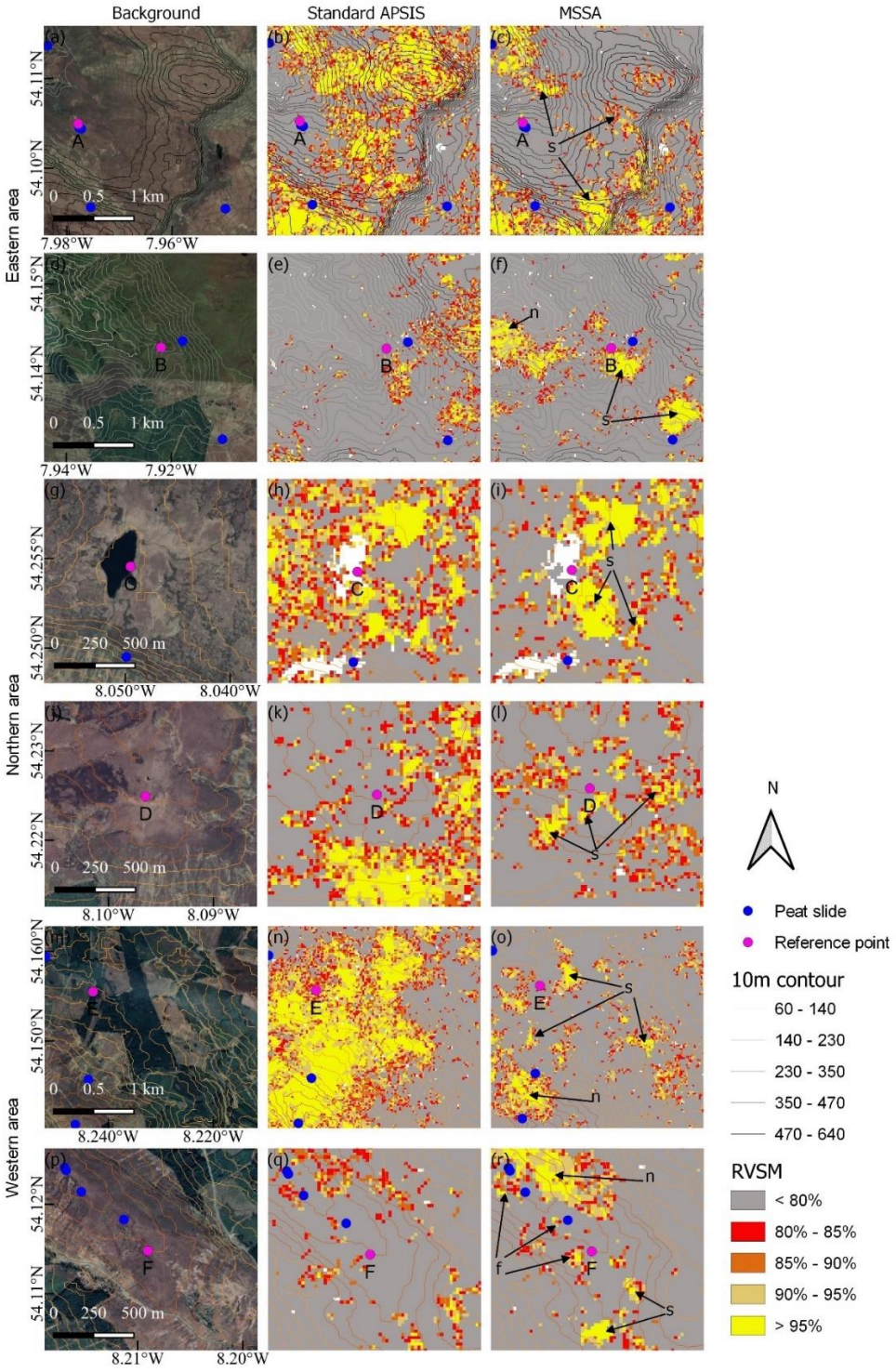

Figure 10. Examples of typical associations between areas of high RVSM and position within a blanket bog landscape. Selected features are chosen from the Eastern (a–f), Northern (g–l) and Western areas (m–r). 10 m topographic contours derived from a DEM are superposed on each image. For each example area the first column is an optical image from Google Earth, the second column is a one-year RVSM image derived from standard APSIS data and the third column is an RVSM image derived from MSSA data. The locations of reference points A–F are shown in Figure 9. Areas of known peat landslide (Geological Survey Ireland 2021) are shown as blue dots. Example landscape associations are shown for associations with seepage (s) at breaks in slope and upslope extension of drainage lines; and associated with peat landslides (f). Note that only the most obvious examples on the optical (Google Earth) image with a N to NE aspect (n) are highlighted.

Shass Mountain which is somewhat similar to the out of phase behaviour between water level and InSAR measures of surface motion observed at a degraded site in the Flow Country (Alshammari *et al.* 2020).

Time series of surface motion also have the capacity to aid evaluation of the processes leading to the landslide event and in non-peat examples have been used to predict failure (Grebby *et al.* 2021). For example, at Shass Mountain a pre-landslide period of low precipitation from April to June caused marked subsidence of the peat surface (Figure 5), potentially causing irreversible deformation of the peat structure ahead of the main landslide event. Similarly, over long periods of time, successive high amplitude oscillations may tend to cumulatively weaken the peat structure, eventually leading to mechanical failure. Translational motion monitoring is also possible and was examined during the course of this research as another product of the stereo calculation required to determine the vertical as opposed to line-of-sight surface motion. However, reliable measurements of lateral motion are limited to the component of movement perpendicular to the satellite path (E–W) and, therefore, cannot be used in a useful way for monitoring large areas. They do however have the potential to add important data to the detailed analysis of suitably orientated landslides. Detailed analysis of these time series is most appropriately undertaken as part of an in-depth site study incorporating field observations either post failure or as part of a detailed site-specific risk assessment.

Comparison of the results from standard APSIS data and MSSA data indicate that both identify areas where the hazard is probably greater (e.g., Figures 4, 9 and 10). However, the MSSA data delineates smaller, better defined areas of potential hazard that more closely align with the known landslides and topographic features in the study sites. Which of these is better is hard to say, as it will depend on how much improvement in hazard classification is sought against the cost of generating the result. Processing times and hence costs are lower for the standard APSIS data. To properly assess the comparable precision of the two methods requires more examples of known landslide - something that can be refined as the number of peat landslides covered by the Sentinel 1 data increases.

Another key finding is that, based on the available data, discrete areas with an enhanced landslide hazard are detectable at least 13–24 months pre failure. This is also supported by the systematic associations between high RVSM and topography, the potential indicators of future peat landslide. Comparison of the RVSM data gathered over six months and one year prior to failure shows little difference in their capacity to identify the same areas. This may be due to the timing of wetting and drying events in a given year; in general, a longer period is more likely to sample the response to a wider range of associated wetting, drying and associated surface motion events.

A limitation at this stage is that our findings are based on three known landslides and more data are required to test, refine and validate our approach. Another uncertainty is how frequently a survey of RVSM should be undertaken and over what period. Ideally, the period should be one with notably variable precipitation that is likely to produce a strong amplitude response.

The method provides precise results using freely available SAR data. Once the InSAR data have been acquired, subsequent processing is rapid and comparatively cheap in terms of computational resources. As such this has the potential to enhance the current hazard mapping by providing an additional level of detail via results that can be visualised graphically and are easily understood by the end-users. We suggest that, following a regional analysis of RVSM based on a period of more than one year, areas with high RVSM should be put into the highest hazard category. This category would merit site investigation ahead of any planned development e.g., road, wind farm, building, etc. As restoration at scale is deployed in the UK and Ireland, RVSM could be used to monitor how different interventions affect surface motion and the risk of landslide, and this would complement the tools currently used for landslide risk assessment which are largely based on slope and peat depth (Scottish Government 2017). For greater consistency, RVSM distributions could be normalised between regions.

ACKNOWLEDGEMENTS

We acknowledge financial support from the University of Nottingham, in particular Professor Sam Kingman. RA and CM are funded by a Leverhulme Research Leadership Award (RL-2019-002). This work stemmed from NERC supported research by DJL, RA, CM and AVB; in particular NERC InSAR TOPS NE/P014100/1 and the NERC Landscape Decisions StAMP NE/T010118/1.

AUTHOR CONTRIBUTIONS

AVB, DJL and MTI conceptualised the research. AVB conducted the MSSA analysis from data

provided by AS. MTI did the statistical modelling and created the Figures and Tables. MTI and DJL wrote the manuscript. AVB, AS, RA, CM, ML, MCB, JC provided additional specialist interpretation, contributed to and reviewed the manuscript.

REFERENCES

Akgun, A., Dag, S., Bulut, F. (2008) Landslide susceptibility mapping for a landslide-prone area (Findikli, NE of Turkey) by likelihood-frequency ratio and weighted linear combination models. *Environmental Geology*, 54(6), 1127–1143. https://doi.org/10.1007/s00254-007-0882-8

Alshammari, L., Boyd, D.S., Sowter, A., Marshall, C., Andersen, R., Gilbert, P., Marsh, S., Large, D.J. (2020) Use of surface motion characteristics determined by InSAR to assess peatland condition. *Journal of Geophysical Research: Biogeosciences*, 125(1), 1–15. https://doi.org/10.1029/2018JG004953

Bateson, L., Cigna, F., Boon, D., Sowter, A. (2015) The application of the Intermittent SBAS (ISBAS) InSAR method to the South Wales Coalfield, UK. *International Journal of Applied Earth Observation and Geoinformation*, 34(1), 249–257. https://doi.org/10.1016/J.JAG.2014.08.018

Berardino, P., Fornaro, G., Lanari, R., Sansosti, E. (2002) A new algorithm for surface deformation monitoring based on small baseline differential SAR interferograms. *IEEE Transactions on Geoscience and Remote Sensing*, 40(11), 2375–2383. https://doi.org/10.1109/TGRS.2002.803792

Bourke, M.C., Thorp, M. (2005) Rainfall-triggered slope failures in eastern Ireland. *Irish Geography*, 38(1), 1–22.

Bradley, A.V., Andersen, R., Marshall, C., Sowter, A., Large, D.J. (2022) Identification of typical eco-hydrological behaviours using InSAR allows landscape-scale mapping of peatland condition. *Earth Surface Dynamics*, 10(2), 261–277. https://doi.org/10.5194/esurf-10-261-2022

Chen, C.W., Zebker, H.A. (2001) Two-dimensional phase unwrapping with use of statistical models for cost functions in nonlinear optimization. *Journal of the Optical Society of America A - Optics Image Science and Vision*, 18(2), 338–351. https://doi.org/10.1364/JOSAA.18.000338

Cigna, F., Sowter, A. (2017) The relationship between intermittent coherence and precision of ISBAS InSAR ground motion velocities: ERS-1/2 case studies in the UK. *Remote Sensing of Environment*, 202, 177–198. https://doi.org/10.1016/J.RSE.2017.05.016

Connolly, J., Holohan, E., Bourke, M., Cruz, C., Farrell, C., Foyle, F., Habib, W., Halpin, R., Henry, T., Hrysiewicz, A., Long, M., Johnson, P., McKeon, C., Trafford, A. (2021) Characterisation of the 2020 Drumkeeran peat landslide: a large peat slide in Ireland. Abstract EGU21-13007, 23rd EGU General Assembly. https://doi.org/10.5194/egusphere-egu21-13007. Online at: https://ui.adsabs.harvard.edu/abs/2021EGUGA..2313007C/abstract

Davies, P.A., McCarthy, M., Christidis, N., Dunstone, N., Fereday, D., Kendon, M., Knight, J.R., Scaife, A.A., Sexton, D. (2021) The wet and stormy UK winter of 2019/2020. *Weather*, 99, 1–7. https://doi.org/10.1002/WEA.3955

Devkota, K.C., Regmi, A.D., Pourghasemi, H.R., Yoshida, K., Pradhan, B., Ryu, I.C., Dhital, M.R., Althuwaynee, O.F. (2013) Landslide susceptibility mapping using certainty factor, index of entropy and logistic regression models in GIS and their comparison at Mugling-Narayanghat road section in Nepal Himalaya. *Natural Hazards*, 65(1), 135–165. https://doi.org/10.1007/s11069-012-0347-6

Dykes, A.P. (2022) Landslide investigations during pandemic restrictions: initial assessment of recent peat landslides in Ireland. *Landslides*, 19, 515–525. https://doi.org/10.1007/s10346-021-01797-0

Dykes, A.P., Jennings, P. (2011) Peat slope failures and other mass movements in western Ireland, August 2008. *Quarterly Journal of Engineering Geology and Hydrogeology*, 44(1), 5–16. https://doi.org/10.1144/1470-9236/09-020

Dykes, A.P., Kirk, K.J. (2001) Initiation of a multiple peat slide on Cuilcagh Mountain, Northern Ireland. *Earth Surface Processes and Landforms*, 26, 395–408. https://doi.org/10.1002/esp.188

Dykes, A.P., Kirk, K.J. (2006) Chapter 16: Slope instability and mass movements in peat deposits. In: Martini, I.P., Cortizas, A.M., Chesworth, W. (eds.) *Peatlands: Evolution and Records of Environmental and Climate Changes*, Developments in Earth Surface Processes 9, Issue C, Elsevier, Amsterdam/Oxford, 377–406. https://doi.org/10.1016/S0928-2025(06)09016-X

Dykes, A.P., Warburton, J. (2007a) Mass movements in peat: A formal classification scheme. *Geomorphology*, 86(1–2), 73–93. https://doi.org/10.1016/J.GEOMORPH.2006.08.009

Dykes, A.P., Warburton, J. (2007b) Significance of geomorphological and subsurface drainage controls on failures of peat-covered hillslopes triggered by extreme rainfall. *Earth Surface Processes and Landforms*, 32(12), 1841–1862. https://doi.org/10.1002/ESP.1499

Dykes, A.P., Warburton, J. (2008) Failure of peat-

covered hillslopes at Dooncarton Mountain, Co. Mayo, Ireland: Analysis of topographic and geotechnical factors. *CATENA*, 72(1), 129–145. https://doi.org/10.1016/J.CATENA.2007.04.008

Farr, T.G., Rosen, P.A., Caro, E., Crippen, R., Duren, R., Hensley, S., Kobrick, M., Paller, M., Rodriguez, E., Roth, L., Seal, D., Shaffer, S., Shimada, J., Umland, J., Werner, M., Oskin, M., Burbank, D., Alsdorf, D. (2007) The shuttle radar topography mission. *Review of Geophysics*, 45, RG2004, 33 pp. https://doi.org/10.1029/2005RG000183

Gee, D., Bateson, L., Sowter, A., Grebby, S., Novellino, A., Cigna, F., Marsh, S., Banton, C., Wyatt, L. (2017) Ground motion in areas of abandoned mining: Application of the Intermittent SBAS (ISBAS) to the Northumberland and Durham Coalfield, UK. *Geosciences*, 7(3), 85, 26 pp. https://doi.org/10.3390/GEOSCIENCES7030085

Geological Survey Ireland (2021) *The Geological Mapping Programme: Spatial Resources*. Online at: https://dcenr.maps.arcgis.com/apps/MapSeries/index.html?appid=a30af518e87a4c0ab2fbde2aaac3c228

Ghil, M., Allen, M.R., Dettinger, M.D., Ide, K., Kondrashov, D., Mann, M.E., Robertson, A.W., Saunders, A., Tian, Y., Varadi, F., Yiou, P. (2002). Advanced spectral methods for climatic time series. *Reviews of Geophysics*, 40(1), 3, 41 pp. https://doi.org/10.1029/2000RG000092

Gong, W., Thiele, A., Hinz, S., Meyer, F.J., Hooper, A., Agram, P.S. (2016) Comparison of small baseline Interferometric SAR processors for estimating ground deformation. *Remote Sensing*, 8(4), 330, 26 pp. https://doi.org/10.3390/RS8040330

Grebby, S., Sowter, A., Gluyas, J., Toll, D., Gee, D., Athab, A., Girindran, R. (2021) Advanced analysis of satellite data reveals ground deformation precursors to the Brumadinho Tailings Dam collapse. *Communications Earth & Environment*, 2, 2, 9 pp. https://doi.org/10.1038/s43247-020-00079-2

Holden, J. (2005) Controls of soil pipe frequency in upland blanket peat. *Journal of Geophysical Research: Earth Surface*, 110(F1), F01002, 11 pp. https://doi.org/10.1029/2004JF000143

Howie, S.A., Hebda, R.J. (2018) Bog surface oscillation (mire breathing): A useful measure in raised bog restoration. *Hydrological Processes*, 32(11), 1518–1530. https://doi.org/10.1002/HYP.11622

Large, D.J., Marshall, C., Jochmann, M., Jensen, M., Spiro, B., Olaussen, S. (2021) Time, hydrologic landscape and the long-term storage of peatland carbon in sedimentary basins. *Journal of Geophysical Research: Earth Surface*, 126(3), e2020JF005762, 15 pp. https://doi.org/10.1002/ESSOAR.10503762.1

Lindsay, R., Bragg, O. (2005) *Wind Farms and Blanket Peat - a Report on the Derrybrien Bog Slide*. Derrybrien Development Cooperative Ltd., Gort, Co. Galway, Ireland, 135 pp. Online at: https://repository.uel.ac.uk/item/867x7

Long, M., Jennings, P. (2006) Analysis of the peat slide at Pollatomish, County Mayo, Ireland. *Landslides*, 3(1), 51–61. https://doi.org/10.1007/s10346-005-0006-z

Long, M., Jennings, P., Carroll, R. (2011) Irish peat slides 2006–2010. *Landslides*, 8(3), 391–401. https://doi.org/10.1007/S10346-011-0254-Z

Marshall, C., Bradley, A.V., Andersen, R., Large, D.J. (2021) *Using Peatland Surface Motion (Bog Breathing) to Monitor Peatland Action Sites*. NatureScot Research Report 1269. Online at: https://www.nature.scot/doc/naturescot-research-report-1269-using-peatland-surface-motion-bog-breathing-monitor-peatland-action#Main+Findings

Met Éireann (2021) *The Irish Meteorological Service - Historical Data*. Online at: https://www.met.ie/climate/available-data/historical-data

Novellino, A., Cigna, F., Brahmi, M., Sowter, A., Bateson, L., Marsh, S. (2017) Assessing the feasibility of a national InSAR ground deformation map of Great Britain with Sentinel-1. *Geosciences*, 7(2), 19, 14 pp. https://doi.org/10.3390/GEOSCIENCES7020019

Osmanoğlu, B., Sunar, F., Wdowinski, S., Cabral-Cano, E. (2016) Time series analysis of InSAR data: Methods and trends. *ISPRS Journal of Photogrammetry and Remote Sensing*, 115, 90–102. https://doi.org/10.1016/J.ISPRSJPRS.2015.10.003

Pradhan, B. (2011) Use of GIS-based fuzzy logic relations and its cross application to produce landslide susceptibility maps in three test areas in Malaysia. *Environmental Earth Sciences*, 63(2), 329–349. https://doi.org/10.1007/s12665-010-0705-1

Price, J.S. (2003) Role and character of seasonal peat soil deformation on the hydrology of undisturbed and cutover peatlands. *Water Resources Research*, 39(9), 1241, 10 pp. https://doi.org/10.1029/2002WR001302

Regmi, N.R., Giardino, J.R., Vitek, J.D. (2010) Modeling susceptibility to landslides using the weight of evidence approach: Western Colorado, USA. *Geomorphology*, 115(1–2), 172–187. https://doi.org/10.1016/j.geomorph.2009.10.002

RPS (2020) *Shass Mountain Peat Landslide: Factual Report*. Report MGE0780RP0001, RPS Group Limited, Mervue, Galway for Department of Culture, Heritage and the Gaeltacht, Dublin, 55 pp. Online at: https://www.npws.ie/sites/default/files/publications/pdf/shass-mountain-landslide-report-october-2020.pdf, accessed 30 Jun 2022.

Ruff, M., Czurda, K. (2008) Landslide susceptibility analysis with a heuristic approach in the Eastern Alps (Vorarlberg, Austria). *Geomorphology*, 94(3–4), 314–324. https://doi.org/10.1016/j.geomorph.2006.10.032

Schreier, G. (1993) *SAR Geocoding: Data and Systems*. Wichmann, Karlsruhe, 435 pp.

Scottish Government (2017) *Peat Landslide Hazard and Risk Assessments: Best Practice Guide for Proposed Electricity Generation Developments*. Second edition, Energy Consents Unit Scottish Government, Edinburgh, 84 pp. Online at: https://www.gov.scot/publications/peat-landslide-hazard-risk-assessments-best-practice-guide-proposed-electricity/documents/

Sowter, A., Bateson, L., Strange, P., Ambrose, K., Fifiksyafiudin, M. (2013) DInSAR estimation of land motion using intermittent coherence with application to the South Derbyshire and Leicestershire coalfields. *Remote Sensing Letters*, 4(10), 979–987. https://doi.org/10.1080/2150704X.2013.823673

Sowter, A., bin Che Amat, M., Cigna, F., Marsh, S., Athab, A., Alshammari, L. (2016) Mexico City land subsidence in 2014–2015 with Sentinel-1 IW TOPS: Results using the Intermittent SBAS (ISBAS) technique. *International Journal of Applied Earth Observation and Geoinformation*, 52, 230–242. https://doi.org/10.1016/J.JAG.2016.06.015

SPECTRA (2021) *SSA-MTM Toolkit for Spectral Analysis*. Online at: http://research.atmos.ucla.edu/tcd/ssa/guide/guide4.html

Thompson, V., Dunstone, N.J., Scaife, A.A., Smith, D.M., Slingo, J.M., Brown, S., Belcher, S.E. (2017) High risk of unprecedented UK rainfall in the current climate. *Nature Communications*, 8 107, 6 pp. https://doi.org/10.1038/s41467-017-00275-3

van den Eeckhaut, M., Hervas, J., Jaedicke, C., Malet, J.P., Montanarella, L., Nadim, F. (2012) Statistical modelling of Europe-wide landslide susceptibility using limited landslide inventory data. *Landslides*, 9(3), 357–369. https://doi.org/10.1007/s10346-011-0299-z

Van Westen, C.J., Rengers, N., Soeters, R. (2003) Use of geomorphological information in indirect landslide susceptibility assessment. *Natural Hazards*, 30(3), 399–419. https://doi.org/10.1023/B:NHAZ.0000007097.42735.9e

Waddington, J.M., Kellner, E., Strack, M., Price, J.S. (2010) Differential peat deformation, compressibility, and water storage between peatland microforms: Implications for ecosystem function and development. *Water Resources Research*, 46(7), W07538, 12 pp. https://doi.org/10.1029/2009WR008802

Warburton, J. (2020) Chapter 9: Peat hazards: compression and failure. In: Giles, D.P., Griffiths, J.S. (eds.) *Geological Hazards in the UK: Their Occurrence, Monitoring and Mitigation*, Engineering Group Working Party Report, Engineering Geology Special Publications 29(1), Geological Society, London, 243–257. http://dx.doi.org/10.1144/EGSP29.9

Warburton, J., Higgitt, D., Mills, A. (2003) Anatomy of a Pennine peat slide, Northern England. *Earth Surface Processes and Landforms*, 28(5), 457–473. https://doi.org/10.1002/ESP.452

Warburton, J., Holden, J., Mills, A.J. (2004) Hydrological controls of surficial mass movements in peat. *Earth-Science Reviews*, 67(1–2), 139–156. https://doi.org/10.1016/J.EARSCIREV.2004.03.003

Winter, T.C. (2000) The vulnerability of wetlands to climate change: A hydrologic landscape perspective. *Journal of the American Water Resources Association*, 36(2), 305–311. https://doi.org/10.1111/J.1752-1688.2000.TB04269.X

Winter, T.C. (2001) The concept of hydrologic landscape perspective. *Journal of the American Water Resources Association*, 37(2), 335–349. https://doi.org/10.1111/J.1752-1688.2001.TB00973.X

Winter, T.C., LaBaugh, J.W. (2003) Hydrologic considerations in defining isolated wetlands. *Wetlands*, 23(3), 532–540.

Submitted 24 Nov 2021, revision 01 Jul 2022
Editor: Olivia Bragg

Author for correspondence: Professor David J. Large, Department of Chemical and Environmental Engineering, Faculty of Engineering, University of Nottingham, Nottingham NG7 2RG, UK.
Tel: +44 115 951 4114; E-mail: david.large@nottingham.ac.uk